An Active Micro Vibration Isolator with Zero-Power Controlled Magnetic Suspension Technology*

Md. Emdadul HOQUE**, Masaya TAKASAKI**, Yuji ISHINO**, Hirohisa SUZUKI** and Takeshi MIZUNO**

In this paper, a three-degree-of-freedom vibration isolation system using active zero-power controlled magnetic suspension is presented in order to isolate vibrations transmitted from the ground and to attenuate the effect of direct disturbances on the table. The zero-compliance of the isolator for direct disturbances was realized by connecting a conventional mechanical spring in series with a negative spring produced by an active magnetic suspension mechanism. In this work, each degree-of-freedom-of-motion of the vibration isolator is treated analytically and it is shown that the developed system is capable to generate infinite stiffness in each mode. Experimental studies have been conducted as well to measure the effectiveness of the isolator under both types of disturbances. Further improvements for the developed system as well as the control techniques are also discussed.

Key Words: Vibration Isolation, Motion Control, Active Vibration Control, Magnetic Bearing, Mode Control, Zero-Power Control, Mechatronics

1. Introduction

In many industrial applications, the need for microvibration isolation has significantly increased in order to achieve high performance for the system. This type of systems should be isolated from ground vibration as well as have capability to suppress the effect of direct disturbance. Since last several decades, conventional passive techniques are used to attenuate the effect of these disturbances[1]. These systems typically pose significant challenges to the conventional passive techniques because lower stiffness of suspension is used for isolating ground vibrations and, in contrast, higher stiffness is necessary for suppressing the effect of direct disturbances[2]. Therefore, a trade-off between them is indispensable to satisfy both demands. Moreover, the performance of the passive techniques is not appropriate enough for high-precision applications.

Active-type vibration isolation systems can overcome this drawback and can be made compatible for both demands. Several researches have been conducted to develop vibration isolation systems using this technique[3]-[6]. However, conventional active-type vibration isolation systems need high-performance sensors such as servo-type accelerometers and external power supply for stable operation. As a result, the systems become rather costlier than the passive-types, and therefore, restrict the application fields of it.

The authors have proposed a unique vibration isolation systems using zero-power magnetic suspension to solve such problems[7]. The proposed vibration isolation system uses only relative displacement sensors which is cheaper than servo-type accelerometers. Since a zero-power system behaves as if it has negative stiffness, infinite stiffness against disturbances on the isolation table can be achieved by combining it with a normal spring. It enables the system to have good characteristics both in reducing vibration transmitted from the floor and in suppressing direct disturbances. A single-axis apparatus was manufactured for basic experimental study[8]. In addition, the system can also be generalized by using a linear actuator instead of hybrid magnet[9].

The purpose of this research is to fabricate a 3-DOF vibration isolator incorporating a single middle table and to propose a mode-based controller for further study. 3-DOF motions of the isolator in the vertical direction are successfully controlled by the proposed method. High stiffness in the three modes are achieved such that direct

* Received 1st February, 2006 (No. 05-4293)

** Department of Mechanical Engineering, Saitama University, 255 Shimo-Okubo, Sakura-ku, Saitama 338-8570, Japan. E-mail: mehoque@mech.saitama-u.ac.jp

disturbance can be suppressed. Transmissibility characteristic of the isolator from the floor have also been measured to demonstrate the isolation performance.

2. Concept of Vibration Isolation System

2.1 Basic principle

Infinite stiffness of a spring can be realized by connecting a normal spring in series with a spring that has negative stiffness. Negative stiffness is generated by using zero-power magnetic suspension, which is discussed in the next section. When two springs with spring constants of k_1 and k_2 are connected in series, the total stiffness k_c is given by

$$k_c = \frac{k_1 k_2}{k_1 + k_2}. \tag{1}$$

This equation shows that the total stiffness becomes lower than that of each spring when normal springs are connected. However, if one of the springs has negative stiffness that satisfies

$$k_1 = -k_2, \tag{2}$$

the resultant stiffness becomes infinite, that is

$$|k_c| = \infty. \tag{3}$$

This research applies this principle of generating high stiffness against direct disturbance to vibration isolation systems. Moreover, if the stiffness of each spring is low enough, the system is capable to isolate floor vibration, as well.

2.2 Zero-power magnetic suspension system

Zero-power magnetic suspension is used to realize negative stiffness. A basic model of single-degree-of-freedom zero-power magnetic suspension using hybrid magnet is shown in Fig. 1. Permanent magnet is used to provide bias flux and the control realizes the steady states in such a way that the electromagnet coil current converges to zero. The attractive force produced by the permanent magnets balances the weight of the suspended object and therefore, the energy consumption for this system is zero in the steady state. The design procedure of the zero-power controller is elaborately discussed in section 4.3. The unique characteristic of the zero-power control system is that it behaves as if it has negative stiffness[10]. Unlike normal mass-spring system where the mass moves to the direction of the applied force when the mass is increased or external force is applied, the suspended object of the zero-power control system moves in the opposite direction in the steady-state as shown in Fig. 2.

2.3 Basic configuration of vibration isolation system

A schematic drawing of the proposed single-degree-of-freedom vibration isolation system using zero-power controlled magnetic suspension is shown in Fig. 3. A middle table m_1 is connected to the base through a spring k_1

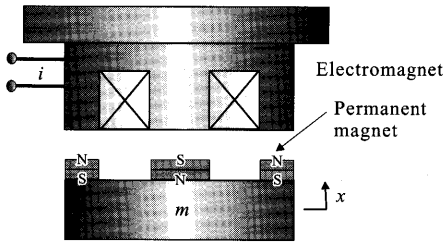

Fig. 1 Basic model of zero-power magnetic suspension

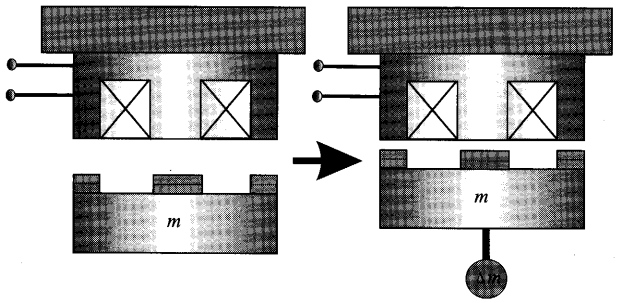

Fig. 2 Characteristic of the zero-power magnetic suspension system

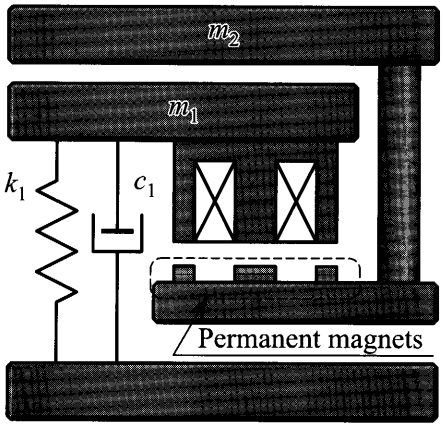

Fig. 3 Structure of the vibration isolator using zero-power magnetic suspension

and a damper c_1 that work as a conventional vibration isolator. An electromagnet for zero-power magnetic suspension is fixed to the middle table. The part of an isolation table m_2 facing the electromagnet is made of soft iron material. The permanent magnet is used to provide bias flux for the zero-power system.

This system can reduce vibration transmitted from the floor by setting k_1 small, and at the same time have infinite stiffness against direct disturbance by setting the amplitude of negative stiffness equal to k_1.

3. Development of MDOF Vibration Isolator

Multi-degree-of-freedom (MDOF) vibration isolator can be developed by utilizing zero-power controlled magnetic suspension system. The proposed vibration isolation system consists of an isolation table, a middle table and a base. The middle table plays a vital role which links a

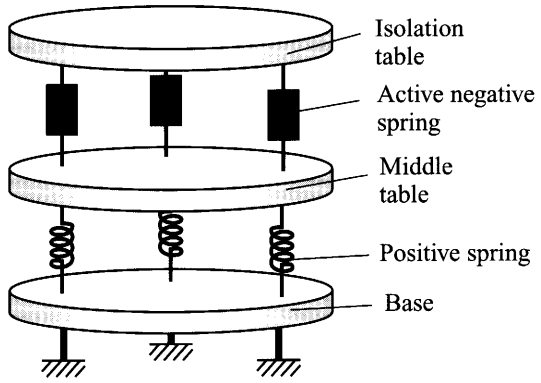

(a) Vibration isolator with concentrated middle mass

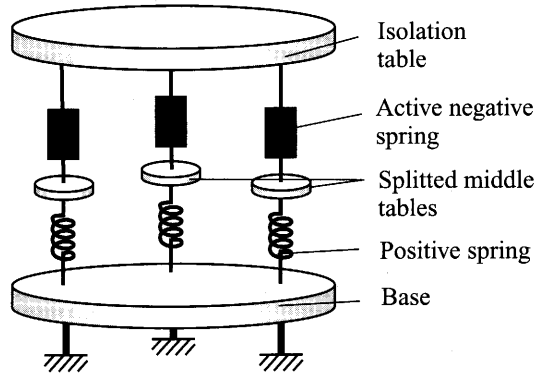

(b) Vibration isolator with modular middle mass

Fig. 4 Proposed conceptual design of multi-axis vibration isolation system

normal spring in series with a magnetic negative spring in such a way that the isolator stiffness is infinite for direct disturbing load and at the same time, the natural frequency of the lower suspension system is set to be low enough for ground vibration. Two types of middle table can be designed for feasible application in developing a multi-degree-of-freedom system. The first one is compact mass or single and concentrated middle table as illustrated conceptually in Fig. 4 (a) and the other is distributed or modular mass as shown in Fig.4 (b). Developing a MDOF system with single middle mass need zero-power controlled magnetic suspension both in the vertical and horizontal directions. Therefore, the whole system becomes complicated and the redundancy of actuators in both directions may occur as well. Hence, the latter type can be used to resolve the above bottlenecks. Six degree-of-freedom vibration isolation system can also be developed using modular middle mass[11]. This system consists of an output link as vibration isolation table, a base and direct acting links. It uses separate unit for controlling each degree-of-freedom motion as a parallel link mechanism. Each direct acting link acts as a single-unit vibration isolation system and therefore, a simplified control technique can be offered, and it may perhaps be a right and proper option for mass productions. However, it poses a challenging task to restrict single-degree-of-freedom motion by a single unit derived from modular middle tables as long as the middle tables are heavy enough or have a sufficient resistance to realize high stiffness for direct disturbance as well as to maintain low natural frequency for ground vibration. Therefore, the former system can be a promising candidate with heavy middle mass to control each degree-of-freedom easily. Moreover, it allows a simplified design of the middle table for the system with more control stability than the latter.

On the other hand, two types of controller can be used to control the three-degree-of-freedom (3-DOF) motions of the isolation system with single middle mass. One is independent or decentralized controller[12] and the other is mode-based or centralized controller[13]. In the former, the coil current of each magnet is controlled on the basis of local information at the corresponding position. In the latter, a controller is designed for each of the modes. In this research, a vibration isolation table with single middle mass has been developed and a mode-based controller is proposed to control the 3-DOF motions.

4. Developed Vibration Isolator

4.1 Structure of the isolator

The anatomized view of the developed vibration isolator using concentrated and single middle mass is illustrated in Fig. 5 (a)[14]. It had a circular isolation table, middle table and base. The height, diameter and mass of the apparatus were 400 mm, 440 mm and 150 kg respectively. The isolation and middle tables weighed 22 kg and 23 kg respectively. Each hybrid magnet for zero-power suspension consisted of a disk-shaped permanent magnet (30×10 mm) and a 2 500-turn electromagnet. The permanent magnet was made of NdFeB materials. The stiffness of each normal spring was 20 N/mm.

The negative stiffness was generated by three hybrid magnets, which suspend the isolation table and were fixed to the middle table. The middle table was suspended by three pairs of spring and actively controlled electromagnets, parallel with the spring, as damper between the base and middle table. It enabled the stiffness and damping characteristics of the positive stiffness to be adjusted flexibly. They were located at the vertices of an equilateral triangle. Each hybrid magnet was aligned with a pair of spring and damper vertically. Hence, the isolation table was suspended by three pairs of normal and negative springs so that the three modes (three-degree-of-freedom motions) of the table can be controlled by the proposed mechanism. They were one translational motion in the vertical direction (Z) and two rotational motions, roll (Θ_x) and pitch (Θ_y).

The relative displacements of the middle table to the base and those of the isolation table to the middle table were detected by six eddy-current gap sensors. The ra-

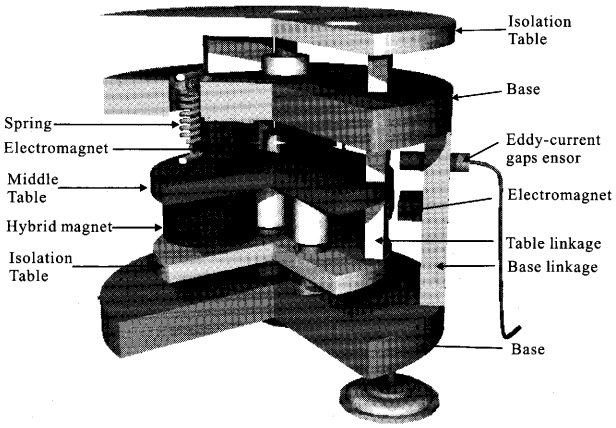

(a) Structure of the developed system

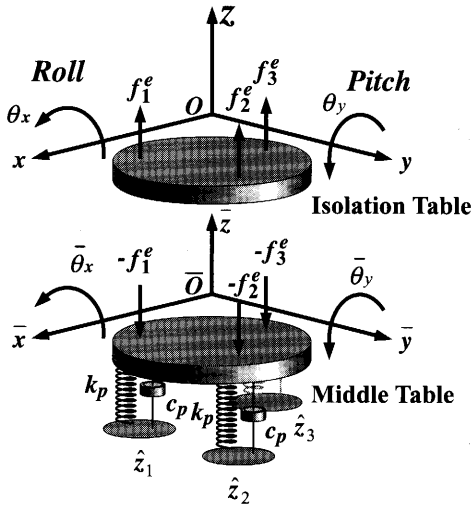

(b) Coordinate system

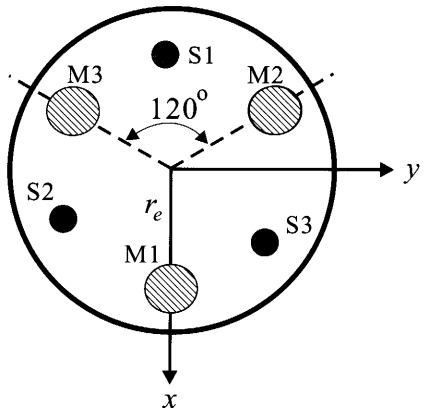

(c) Layout of Sensors (S) and hybrid magnets (M)

Fig. 5 Schematic (anatomized) diagram of the vibration isolator

dial displacements of the isolation table were measured by another three gap sensors and radial motions of the table were actively controlled.

4.2 Model

The schematic diagram of the coordinate system is shown in Fig. 5 (b) and the layout of sensors and hybrid magnets is shown in Fig. 5 (c). It is assumed that the roll and pitch angles are so small that $\cos\theta_x \cong 1$, $\sin\theta_x \cong \theta_x$, $\cos\theta_y \cong 1$ and $\sin\theta_y \cong \theta_y$, where θ_x, θ_y: roll and pitch angles of the isolation table. The equations of motion of the isolation table for vertical translation, roll and pitch modes respectively can be written as

$$m\ddot{z} = f_z^e + f_z^d, \tag{4}$$

$$J_x\ddot{\theta}_x = m_x^e + m_x^d, \tag{5}$$

and

$$J_y\ddot{\theta}_x = m_y^e + m_y^d, \tag{6}$$

where

m : mass of isolation table,
J_x : inertial momentum of isolation table about x-axis,
J_y : inertial momentum of isolation table about y-axis,
z : displacement of the center of isolation table,
f_z^e : z-direction total force by the hybrid magnets,
m_x^e : total moment about x-axis by the hybrid magnets,
m_y^e : total moment about y-axis by the hybrid magnets,
f_z^d : z-direction direct disturbance,
m_x^d : direct disturbance about the x-axis,
m_y^d : direct disturbance about the y-axis.

The force of each magnet is approximately given by

$$f_k^e = k_s g_k + k_i i_k \quad (k = 1,2,3), \tag{7}$$

where

g_k : deviation of the gap between the electromagnet and the target on the isolation table,
i_k : control current.

It is found that the dynamics of the three modes for isolation table can be treated separately and, in addition, equation of motions for vertical translation, roll and pitch modes respectively can be written as

$$m\ddot{z} = 3k_s(z - \bar{z}) + k_i(i_1 + i_2 + i_3) + f_z^d, \tag{8}$$

$$J_x\ddot{\theta}_x = \frac{3}{2}r_e^2 k_s(\theta_x - \bar{\theta}_x) + \frac{\sqrt{3}}{2}r_e k_i(i_2 - i_3) + m_x^d, \tag{9}$$

$$J_y\ddot{\theta}_y = \frac{3}{2}r_e^2 k_s(\theta_y - \bar{\theta}_y) + \frac{1}{2}r_e k_i(-2i_1 + i_2 + i_3) + m_y^d, \tag{10}$$

where

$\bar{z}$: displacement of the center of the middle table,
r_e : distance of the hybrid magnets from the center,
$\bar{\theta}_x$: roll angle of the middle table,
$\bar{\theta}_y$: pitch angle of the middle table.

4.3 Control system design

4.3.1 Basic zero-power control system The zero-power control system is described by using the model shown by Fig. 1. The suspended object with mass of m is assumed to move only in the vertical translational direction. The equation of motion for the model is given by

$$m\ddot{x} = k_s x + k_i i + f_d, \tag{11}$$

where

x : displacement of the suspended object,
k_s : gap-force coefficient of the magnet,
k_i : current-force coefficient of the magnet,
i : control current of the electromagnet,
f_d : disturbance acting on the suspended object.

The transfer function representation of the dynamics described by Eq. (11) becomes

$$X(s)=\frac{1}{s^2-a_0}[b_0I(s)+d_0F_d(s)], \tag{12}$$

where each Laplace-transformed variable is denoted by its capital, and

$$a_0=\frac{k_s}{m},\quad b_0=\frac{k_i}{m},\quad d_0=\frac{1}{m}.$$

The zero-power control operates to accomplish

$$\lim_{t\to\infty} i(t)=0 \quad \textit{for} \text{ stepwise disturbances.} \tag{13}$$

The zero-power controller is generally represented by[10]

$$I(s)=-\frac{sh(s)}{g(s)}X(s), \tag{14}$$

where $g(s)$ and $h(s)$ are coprime polynomial in s and selected for the closed-loop systems to be stable, that is, all the roots of the characteristic equation

$$t_c(s)=(s^2-a_0)g(s)+b_0h(s)=0, \tag{15}$$

are in the left-hand plane.

In discussing zero-power control, therefore, the disturbance should be considered to be stepwise.

$$F_d(s)=\frac{F_0}{s}. \tag{16}$$

To achieve the control object in Eq. (14), $h(s)$ must satisfy

$$h(s)=s\tilde{h}(s), \tag{17}$$

where $\tilde{h}(s)$ is an appropriate polynomial. Assuming that $h(s)/g(s)$ in Eq. (14) is restricted to be proper, the minimal order compensator achieving zero-power control and assigning the closed-loop poles arbitrarily can be represented as

$$I(s)=-\frac{s(\tilde{h}_2s+\tilde{h}_1)}{s^2+g_1s+g_0}X(s). \tag{18}$$

From Eq. (18), the characteristic polynomial of the closed-loop system is obtained as[13]

$$t_c(s)=s^4+g_1s^3+(-a_0+g_0+b_0\tilde{h}_2)s +(-a_0g_1+b_0\tilde{h}_1)s-a_0g_0. \tag{19}$$

Assuming that the characteristic polynomial specifying the desired location of the roots is

$$t_d(s)=(s^2+2\zeta_1\omega_1s+\omega_1^2)(s^2+2\zeta_2\omega_2s+\omega_2^2). \tag{20}$$

The coefficients of g_i's and h_i's of the controller of Eq. (18) are determined uniquely by comparing the coefficients in Eqs. (19) and (20).

The zero-power controller as described in Eq. (18) can also be realized by combining a PD control and a local integral feedback of current in the hybrid magnet as

$$i=-\left(p_d+p_v\frac{s}{Ts+1}\right)g+\frac{p_i}{s}i, \tag{21}$$

where

p_d : displacement feedback gain,
p_v : velocity feedback gain,
T^{-1} : cut-off frequency (rad) of the pseudo differentiator,
g : relative displacement of the isolation table from the base,
p_i : current-integral feedback gain.

From Eq. (21), it can be written as

$$I(s)=-s\frac{(p_d+p_v)s+(p_dT^{-1})}{s^2+(T^{-1}-p_i)s-T^{-1}p_i}G(s)=-sc_2(s)G(s), \tag{22}$$

where $c_2(s)$ corresponds to $h(s)/g(s)$ in Eq. (14) and $\frac{\tilde{h}_2s+\tilde{h}_1}{s^2+g_1s+g_0}$ in Eq. (18).

4.3.2 Controller for 3-DOF system The developed vibration isolation system is a three-channel MIMO system. The zero-power controller for Z, Θ_x and Θ_y modes are designed respectively to have such dynamics as Eq. (18)

$$I^Z(s)=-\frac{s(\tilde{h}_2^Zs+\tilde{h}_1^Z)}{s^2+g_1^Zs+g_0^Z}Z(s)=-sc_2^Z(s)Z(s), \tag{23}$$

$$I^{\Theta_x}(s)=-\frac{s(\tilde{h}_2^{\Theta_x}s+\tilde{h}_1^{\Theta_x})}{s^2+g_1^{\Theta_x}s+g_0^{\Theta_x}}\Theta_x(s)=-sc_2^{\Theta_x}(s)\Theta_x(s), \tag{24}$$

$$I^{\Theta_y}(s)=-\frac{s(\tilde{h}_2^{\Theta_y}s+\tilde{h}_1^{\Theta_y})}{s^2+g_1^{\Theta_y}s+g_0^{\Theta_y}}\Theta_y(s)=-sc_2^{\Theta_y}(s)\Theta_y(s). \tag{25}$$

The coefficient of each mode was determined from the system characteristics. Designed control algorithms were implemented with a digital controller DS1103 supplied by dSPACE^{TM}. The sampling rate was 10 kHz.

4.4 Response to direct disturbance

The initial values are assumed to zero for simplicity. From Eqs. (8) and (23) for Z- mode, displacement of the isolation table can be written as

$$Z(s)=\frac{(3c_ps+3k_p)(k_ic_2^Z(s)s-3k_s)}{t_c(s)}\hat{Z}(s) +\frac{t_1(s)+k_ic_2^Z(s)s-3k_s}{t_c(s)}F_d(s), \tag{26}$$

where

$$t_1(s)=\bar{m}s^2+3c_ps+3k_p, \tag{27}$$

$$t_2(s)=ms^2+k_ic_2^Z(s)s-3k_s, \tag{28}$$

$$t_c(s)=t_1(s)t_2(s)+ms^2(k_ic_2^Z(s)s-3k_s), \tag{29}$$

$\hat{Z}=\sum\frac{Z_k}{3}$ = displacement of the center of base $(k=1,2,3)$,
c_p = damping constant of the damper,
k_p = stiffness of the normal spring.

To estimate the stiffness for direct disturbance, F_d is assumed to be stepwise as described in Eq. (16). When the

vibration of the floor is neglected, the steady-state displacement of the table is obtained as

$$\frac{Z(\infty)}{F_0}=\lim_{s\to 0}\frac{ms^2+(3c_p+k_ic_2^Z(s))s+3k_p-3k_s}{t_c(s)}$$
$$=\frac{1}{3k_p}-\frac{1}{3k_s}, \tag{30}$$

Therefore

$$\frac{Z(\infty)}{F_0}=0, \tag{31}$$

when

$$k_p=k_s. \tag{32}$$

It is shown in Eq. (31) that the displacement of the isolation table for any stepwise direct load in the vertical translational direction is zero. In similar way, when Eq. (32) is satisfied, the static displacements become zero as well for roll and pitch modes. Therefore, the suspension system between the isolation table and the floor would have infinite stiffness for direct disturbing load.

5. Experimental Result

Several experiments were carried out to measure the performance of the controller designed for the isolator. First, the static and dynamic responses of the isolator to direct disturbance were measured, and finally, the absolute transmissibility of the isolator from the base was measured to investigate the floor vibration isolation performances.

5.1 Static response to direct disturbance

The static response of the isolator from the base to direct disturbance in three modes is shown in Fig. 6. The load was added to the center of the isolation table for vertical translational mode and on the y- and x-axis (150 mm away from the center) for roll and pitch modes respectively. It is observed from the figures that the table maintained almost same position, while the position of the middle table changed proportional to the load applied for all the three modes.

5.2 Dynamic response to direct disturbance

Figure 7 shows the step responses of the developed isolator. In this experiment, a load (14.7 N) was added to the center of the isolation table and then, suddenly removed from the isolation table to generate stepwise disturbance. The response was measured at the same point. The close-loop poles of the zero-power controller were selected by choosing the design frequency ($\omega_1=\omega_2=\omega$) as

(a) $2\pi\times4$ [1/s]
(b) $2\pi\times5$ [1/s]
(c) $2\pi\times6$ [1/s],

in Eq. (20) while the damping ratio ($\zeta_1=\zeta_2=\zeta$) was fixed to 1.0. It is seen from Fig. 7 (a) that when the load was removed, the table moved upward in the direction of the load removal and the table returned to the original position after a certain period. When the higher closed-loop poles were assigned, the displacement of the isolation table, as well as the time required for the table to return to the original position were reduced, as shown in Fig. 7 (b) and (c). It is clear that the dynamic characteristic of the isolator was improved by selecting the higher closed-loop poles of the zero-power controller.

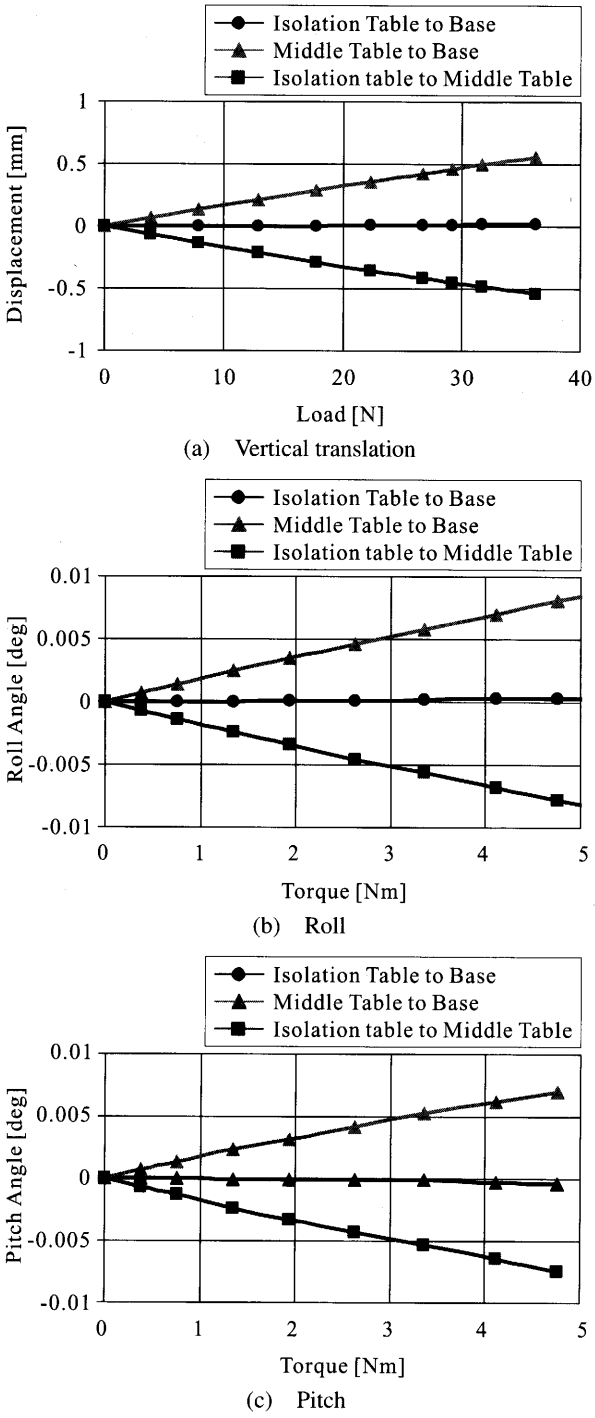

(a) Vertical translation
(b) Roll
(c) Pitch

Fig. 6 Static response of the isolator to direct disturbances in the three modes

Figure 8 shows the dynamic response of the isolation table at low frequency. In this case, the table was excited by two voice coil motors at 0.015 Hz in the z-direction

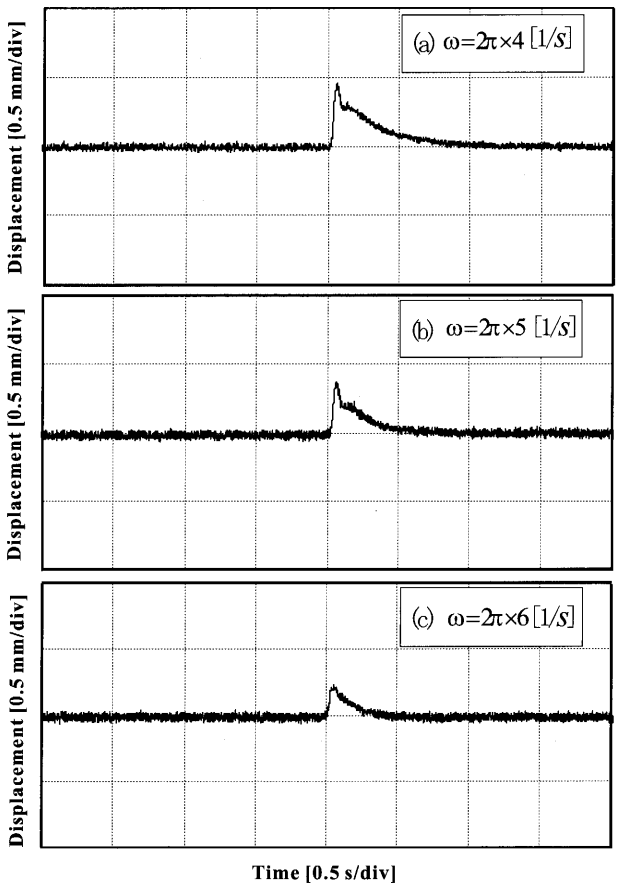

Fig. 7 Step responses of the developed isolator

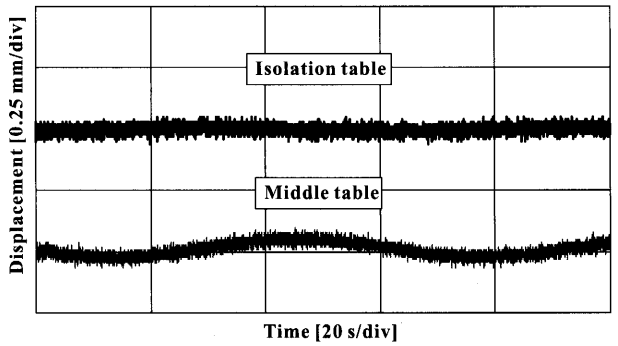

Fig. 8 Dynamic response of the isolation table at low frequency

which were fixed to the base, and the response of the table was measured at the center of the table. The results show that middle table was displaced from the original position while the isolation table remained almost in the same position. The maximum displacement of the isolation table was 5 μm at the peak while that of the middle table was 33 μm. The response of the isolation table to moving mass is presented in Fig. 9. A rolling mass (1.5 kg) was moved in this experiment from one end of the isolation table to the other in the pitch mode trajectory, and the position of the isolation table and the middle table was measured in that direction. The displacement was measured by sensor placed at 85 mm off the center in the pitch mode trajectory as shown in Fig. 5 (c). It is obvious from the figure that the isolation table generated very high stiffness such that its position remained almost in the original state in the course of the mass movement.

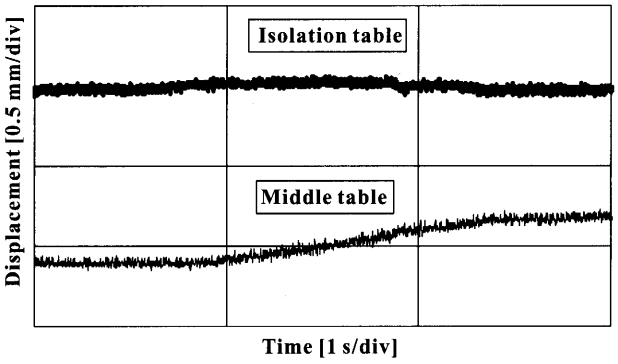

Fig. 9 Response of the isolation table to moving mass

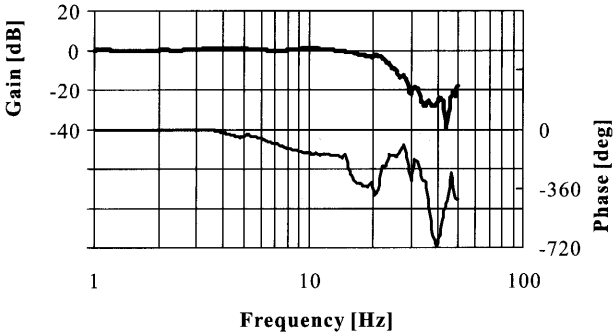

Fig. 10 Absolute transmissibility of the isolator from the floor during floor excitation

5.3 Ground vibration isolation

Finally, the absolute transmissibility of the isolator ($z/\hat{z}$) was measured by vibrating the base of the apparatus vertically by a pneumatic actuator and measuring the response of the table at the center, as shown in Fig. 10. The experiments were carried out by changing the damping coefficients of the damper electromagnet located between the base and the middle table. The resonance peak was appeared at 7.33 Hz in case of lower damping. In the experiment, the damping coefficient ($c_p = 0.8$) was selected by trial and error method. The closed-loop poles of the zero-power controller for Z-mode was selected as $\omega(=\omega_1=\omega_2)=2\pi\times3$ [1/s] and ζ ($=\zeta_1=\zeta_2$) =1.4. The result shows that the isolator can suppress the resonance peak efficiently and have ability to insulate ground vibrations.

6. Conclusion

An active microvibration isolator using zero-power controlled magnetic suspension technology was developed and a mode-based control strategy was proposed. The experimental results demonstrated well that the developed isolator could realize high stiffness against static direct disturbances in the three modes. The dynamic per-

formance of the isolator was also demonstrated by applying stepwise disturbances and exciting the table at low frequency. The dynamic performance of the isolator could be improved by selecting proper closed-loop poles of the zero-power controller. The transmissibility characteristic of the isolator from the floor showed that it was capable to suppress the resonance peak effectively during floor excitation. The zero-power control system has nonlinearity due to the strong nonlinear magnetic force and therefore, the direct disturbance suppression performance can further be improved by using linearized zero-power control. Furthermore, to meet the growing demands to support heavy payload on the isolation table, a weight support mechanism can be used. The proposed system will downscale the design intricacy and system development cost.

Acknowledgment

The authors gratefully acknowledge the financial support provided for this project from the Ministry of Education, Culture, Sports, Science and Technology of Japan, and Electro-Mechanic Technology Advancing Foundation as a Grant-in-Aid for the Development of Innovative Technology and a Grant-in-Aid for Scientific Research (B).

References

(1) Ho, S.T., Matsuhisa, H. and Honda, Y., Passive Vibration Suppression of Beam with Piezoelectric Elements, JSME Int. J., Ser.C, Vol.43, No.3 (2000), pp.740–747.

(2) Rivin, E.I., Passive Vibration Isolation, (2003), ASME Press, New York.

(3) Yasuda, M. and Ikeda, M., Double-Active Control of Microvibration Isolation Systems to Improve Performances (Application of Two-Degree-of-Freedom Control), Trans. Jpn. Soc. Mech. Eng., (in Japanese), Vol.59, No.562, C (1993), pp.1694–1701.

(4) Yoshioka, H., Takahashi, Y., Katayama, K., Imazawa, T. and Murai, N., An Active Microvibration Isolation System for Hi-Tech Manufacturing Facilities, ASME Journal of Vibration and Acoustics, Vol.123 (2001), pp.269–275.

(5) Yasuda, M., Osaka, T. and Ikeda, M., Feed Forward Control of a Vibration Isolation System for Disturbance Suppression, Proc. of the 35th Conference on Decision and Control, Kobe, Japan, (1996), pp.1229–1233.

(6) Watanabe, K., Hara, S., Kanemitsu, Y., Haga, T., Yano, K., Mizuno, T. and Katamura, R., Combination of H^{∞} and PI Control for an Electromagnetically Levitated Vibration Isolation System, Proc. 35th IEEE Conference on Decision and Control, Kobe, Japan, (1996), pp.1223–1228.

(7) Mizuno, T., Proposal of a Vibration Isolation System Using Zero-Power Magnetic Suspension, Proc. Asia-Pacific Vibration Conference 2001, Vol.2 (2001), pp.423–427.

(8) Mizuno, T., Vibration Isolation System Using Zero-Power Magnetic Suspension, Preprints of 15th World Congress of the IFAC, Spain, (2002), Paper No. 955.

(9) Mizuno, T., Toumiya, T. and Takasaki, M., Vibration Isolation System Using Negative Stiffness, JSME Int. J., Ser.C, Vol.46, No.3 (2003), pp.807–812.

(10) Mizuno, T. and Takemori, Y., A Transfer-Function Approach to the Analysis and Design of Zero-Power Controllers for Magnetic Suspension System, Electrical Engineering in Japan, Vol.141, No.2 (2002), pp.933–940.

(11) Ishigami, T., Takasaki, M., Ishino, Y., Hoque, M.E., Mizuno, T. and Toumiya, T., Proposal of an Active Vibration Isolation System with a Parallel Mechanism Using Zero-Power Magnetic Suspension, CD-ROM Proc. 7th International Conference on Motion and Vibration Control (MOVIC 04), USA, (2004), Paper No.134.

(12) Mizuno, T., Takasaki, M., Suzuki, H. and Ishino, Y., Development of a Three-Axis Active Vibration Isolation System Using Zero-Power Magnetic Suspension, Proc. 42nd IEEE Conference on Decision and Control, Hawaii, USA, December, (2003), pp.4493–4498.

(13) Hoque, M.E., Takasaki, M., Ishino, Y. and Mizuno, T., Design of a Mode-Based Controller for 3-DOF Vibration Isolation System, Proc. 2004 IEEE Conference on Robotics, Automation and Mechatronics, Singapore, December, (2004), pp.478–483.

(14) Hoque, M.E., Takasaki, M., Ishino, Y. and Mizuno, T., Development of a Three-Axis Active Vibration Isolator Using Zero-Power Control, IEEE/ASME Transactions on Mechatronics, Vol.11, No.4 (2006), pp.461–469.